INL/EXT-21-65160

Bison As-run AGR-3/4 Irradiation Test Predictions

November 2021

William F. Skerjanc
Wen Jiang

Idaho National Laboratory

INL is a U.S. Department of Energy National Laboratory operated by Battelle Energy Alliance, LLC

INL/EXT-21-65160

Bison As-run AGR-3/4 Irradiation Test Predictions

William F. Skerjanc
Wen Jiang

November 2021

Idaho National Laboratory
Advanced Reactor Technologies
Idaho Falls, Idaho 83415

http://www.art.inl.gov

Prepared for the
U.S. Department of Energy
Office of Nuclear Energy
Under DOE Idaho Operations Office
Contract DE-AC07-05ID14517

Page intentionally left blank

INL ART Program

Bison As-run AGR-3/4 Irradiation Test Predictions

INL/EXT-21-65160

November 2021

Technical Reviewer:

Jason D. Hales Computational Mechanics and Materials Manager	15 November 2021 Date

Approved by:

Paul A. Demkowicz AGR Fuels Technical Director	11/15/2021 Date
Gerhard Strydom INL ART Director	11/15/2021 Date
Michelle T. Sharp INL Quality Assurance	11/15/2021 Date

ABSTRACT

Bison, a nuclear fuel performance application built using the Multiphysics Object-Oriented Simulation Environment (MOOSE) finite element library, was used to model the Advanced Gas Reactor (AGR)-3/4 irradiation test using as-run physics and thermal hydraulics data. The AGR-3/4 test consists of the combined third and fourth planned irradiations of the AGR Fuel Development and Qualification Program. The AGR-3/4 test train consists of 12 separate and independently controlled and monitored capsules. Each capsule contains four compacts filled with both uranium oxycarbide (UCO) unaltered "driver" fuel particles and UCO designed-to-fail (DTF) fuel particles. This report documents the calculations performed to predict the failure probability of tristructural isotropic (TRISO)-coated driver fuel particles during the AGR-3/4 experiment on a single compact. This report will demonstrate the capabilities of Bison to model the complex AGR-3/4 irradiation test and identify further development needed to capture the fuel particle failure probability and source term on every compact for further comparison from post-irradiation examination (PIE) data. The calculations include the modeling of the AGR-3/4 irradiation that occurred from December 2011 to April 2014 in the Advanced Test Reactor (ATR) over a total of 10 ATR cycles including seven normal cycles, one low-power cycle, one unplanned outage cycle, and one power axial locator mechanism (PALM) cycle.

Page intentionally left blank

CONTENTS

FIGURES

TABLES

Page intentionally left blank

ACRONYMS

AGR	Advanced Gas Reactor
ATR	Advance Test Reactor
DTF	designed-to-fail
EFPD	effective full power days
FIMA	fissions per initial heavy metal atom
HTGR	high-temperature gas-cooled reactor
INL	Idaho National Laboratory
IPyC	inner pyrolytic carbon
LEU	low-enriched uranium
MOOSE	Multiphysics Object-Oriented Simulation Environment
NEFT	Northeast Flux Trap
OPyC	outer pyrolytic carbon
PALM	Power Axial Locator Mechanism
PARFUME	PARticle FUel ModEl
PIE	post-irradiation examination
SiC	silicon carbide
TAVA	time-average/volume-average
TRISO	tristructural isotropic
UCO	uranium oxycarbide

Page intentionally left blank

Bison As-Run AGR-3/4 Irradiation Test Predictions

1. INTRODUCTION

Several fuel and material irradiation experiments have been planned for Idaho National Laboratory's (INL's) Advanced Reactor Technologies (ART) Advanced Gas Reactor (AGR) Fuel Development and Qualification Program (referred to as the INL ART/AGR fuel program hereafter). These experiments support development and qualification of tristructural isotropic (TRISO)-coated particle fuel for use in high-temperature gas-cooled reactors (HTGRs). The goals of these experiments are to provide irradiation performance data to support fuel process development, qualify fuel for normal operating conditions, support development and validation of fuel performance and fission product transport models and codes, and provide irradiated fuel and materials for post-irradiation examination (PIE) and safety testing (Demkowicz 2021). AGR-3/4 combined the third and fourth in this series of planned experiments to test TRISO-coated, low-enriched uranium (LEU) oxycarbide (UCO) fuel.

This report documents the calculations performed to predict the failure probability of TRISO-coated fuel particles during the AGR-3/4 experiment along with the source term from a single compact using Bison (Williamson et al. 2021). In addition, this report will demonstrate the capabilities of Bison to model the complex AGR-3/4 irradiation test and identify further development needed to capture the fuel particle failure probability and source term on every compact for further comparison from PIE data. The calculations include modeling AGR-3/4 compacts irradiated from December 2011 to April 2014 in the Advanced Test Reactor (ATR) over a total of 10 ATR cycles, including seven normal cycles, one low-power cycle, one unplanned outage cycle, and one power axial locator mechanism (PALM) cycle for a total of 369.1 effective full power days (EFPD). Because no burnup was accumulated during the low-power cycle and the AGR-3/4 test train was moved to the ATR canal during the unplanned outage and PALM cycles, the modeling covers only the seven normal power cycles. Previously, INL's fuel performance code PARticle FUel ModEl (PARFUME) was used to predict fuel performance for the AGR-3/4 irradiation experiment (Skerjanc 2016).

The AGR-3/4 fuel test has been successfully completed, and the results are presented in the AGR-3/4 Irradiation Test Final As-Run Report (Collin 2015). Final burnup values on a per compact basis ranged from 4.85 to 15.27% fissions per initial heavy metal atom (FIMA), while fast fluence values ranged from 1.19 to 5.32×10^{25} n/m^2 ($E_n > 0.18$ MeV). Time-average/volume-average (TAVA) fuel temperatures on a capsule basis at the end of irradiation ranged from 845°C in Capsule 12 to 1276°C in Capsule 7.

Details associated with completing these calculations are provided in the remainder of this document. The AGR-3/4 irradiation experiment description is briefly introduced in Section 2, Bison modeling is outlined in Section 3, results are described in Section 4, conclusions are given in Section 5, and references are listed in Section 6.

1.1 AGR Program

The Department of Energy (DOE) AGR Fuel Development and Qualification program was established to qualify TRISO-coated fuel for use in HTGRs. The primary goal of the program is to provide a baseline fuel qualification data set in support of the licensing and operation of a HTGR (Demkowicz 2021).

Seven fuel and material irradiation experiments were planned for the DOE AGR program. The overall objectives of these experiments are to (Demkowicz 2021):

•Develop fuel fabrication capabilities

•Perform fuels and materials irradiation

•Perform safety testing and PIE

•Improve fuel performance modeling

•Evaluate fission product transport and source term determination.

1.2 Bison

Bison (Williamson 2021) is a nuclear fuel performance application built using the Multiphysics Object-Oriented Simulation Environment (MOOSE) finite element library (Permann et al. 2020) developed at INL. Bison is capable of modeling multiple fuel forms in a wide variety of dimensions and geometries. It solves coupled nonlinear partial differential equations, including heat conduction, mechanics, fission product species transport, etc., in a fully implicit manner. More detailed descriptions of the Bison fuel performance code as it relates to TRISO fuel modeling can be found in "Bison TRISO Modeling Advancements and Validation to AGR-1 Data" (Hales 2020) and "TRISO particle fuel performance and failure analysis with Bison" (Jiang et al. 2021).

Different irradiation conditions can be easily incorporated in Bison simulations. Bison has the capability to run either very small analyses with a single processor or very large analyses on multiple processors on a supercomputer. For TRISO fuel, Bison supports spherically symmetric models, axisymmetric models, and fully 3D models. Thermo-mechanical models for each material layer includes elastic, irradiation creep, irradiation-induced dimension change, thermal expansion, and thermal conductivity.

Fission product generation, diffusion, and release can also be modeled for TRISO particles with uranium dioxide (UO_2) and UCO kernels. In addition, Bison has the ability to perform statistical failure analysis of large samples of fuel particles. This capability enables evaluation of failure due to multidimensional failure phenomena by analyzing many thousands of particles. This enables realistic calculations of fission product release from the many particles in a TRISO-fueled reactor.

2. AGR-3/4 IRRADIATION EXPERIMENT

As defined in the technical program plan for the INL ART/AGR fuel program (Demkowicz 2021), the objectives of the AGR-3/4 experiment are as follows:

1. Irradiate fuel containing UCO designed-to-fail (DTF) fuel particles that will provide a known source of fission products for subsequent transport through compact matrix and structural graphite materials
2. Assess the effects of sweep gas impurities (such as CO, H_2O, and H_2) that are typically found in the primary coolant circuit of HTGRs, on fuel performance and subsequent fission product transport
3. Provide irradiated fuel and material samples for PIE and safety testing
4. Support the refinement of fuel performance and fission product transport models with online, PIE, and safety test data.

2.1 Fuel Characteristics

Fuel for AGR-3/4 contained conventional driver fuel that was similar to the baseline fuel used in the AGR-1 experiment (Barnes 2006a) and the DTF fuel particles whose kernels were identical to the driver fuel kernels and whose coatings were DTF under irradiation, leaving fission products to migrate through the surrounding materials (Barnes 2006b; Marshall 2011):

- Driver fuel consisted of TRISO-coated particles that were slightly less than 1 mm in diameter. Each particle had a central reference kernel that contains fuel material, a porous carbon buffer layer, an inner pyrolytic carbon (IPyC) layer, a silicon carbide (SiC) barrier coating, and an outer pyrolytic carbon (OPyC) layer as depicted in Figure 1. Each layer's function is described in Table 1. Kernels for AGR-3/4 consists of UCO fuel.

- DTF fuel consisted of reference kernels with a 20-µm thick pyrolytic carbon seal coating. This coating was DTF early in the irradiation and provide a known source of fission products.

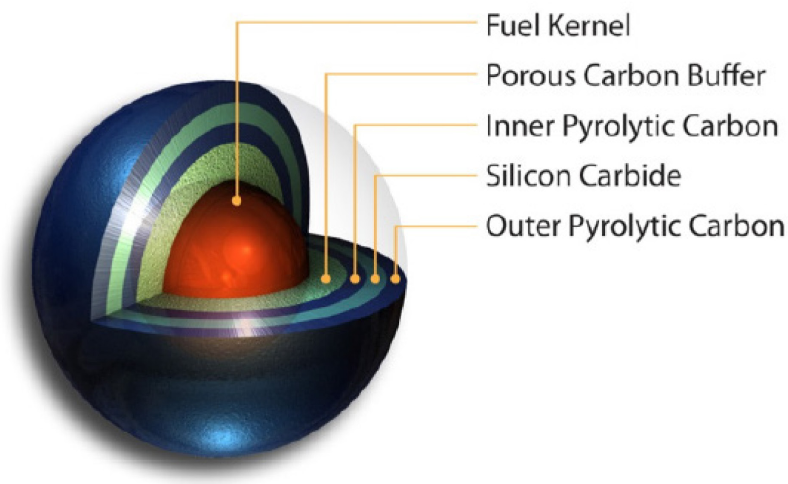

Figure 1. Typical TRISO-coated fuel particle.

Table 1. Primary functions of particle fuel components.

Component	Primary Function
Kernel	Contains fissile fuel.
Buffer	Provides void space for fission product gases and accommodates differential changes in dimensions between coating layers and kernel.
IPyC	Structural layer and fission gas barrier that protects the kernel during SiC deposition and the SiC layer from most fission products during irradiation.
SiC	Primary structural layer and primary fission product barrier.
OPyC	Structural layer that also permits embedding the particles in graphitic matrix material.

Kernels for AGR-3/4 consisted of LEU UCO fuel. The kernels were fabricated by BWX Technologies (BWXT 2006) in accordance with the AGR-3/4 DTF Fuel and Capsule Component Material Specifications (Marshall 2011). The UCO kernels were coated and characterized by Oak Ridge National Laboratory (Hunn 2007; Hunn 2011). Coating was performed in accordance with the AGR-3/4 fuel product specification (Barnes 2006b; Marshall 2011).

After coating, AGR-3/4 fuel was formed into right cylindrical compacts. The compact matrix material was composed of a thermosetting carbonaceous material. Prior to compacting, the fuel particles were overcoated with thick layers of the compact matrix material. This overcoat was intended to prevent particle-to-particle contact and help achieve the desired packing fraction of the fuel particles. Each AGR-3/4 compact contained driver fuel particles and 20 DTF particles (about 1% of the particles) that were placed along its axis (Figure 2). AGR-3/4 compacts were nominally 12.51 mm in length and 12.31 mm in diameter. A complete description of the fuel compacts, fission product monitoring system, physics analysis, and thermal analysis were presented in the final as-run report (Collin 2015).

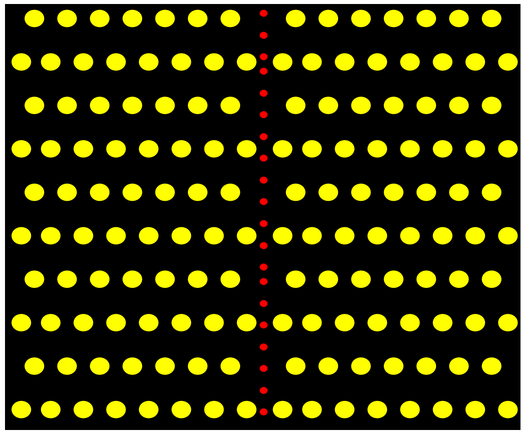

Figure 2. Schematic of an AGR-3/4 compact with DTF fuel particles along the axis.

2.2 AGR-3/4 Description

To achieve the test objectives outlined above, in accordance with requirements from the technical program plan (Demkowicz 2021) and the irradiation test specification (Maki 2011), AGR-3/4 was irradiated in the northeast flux trap (NEFT) position of the ATR at INL. A cross-sectional view of the ATR core, which indicates the NEFT location, is displayed in Figure 3.

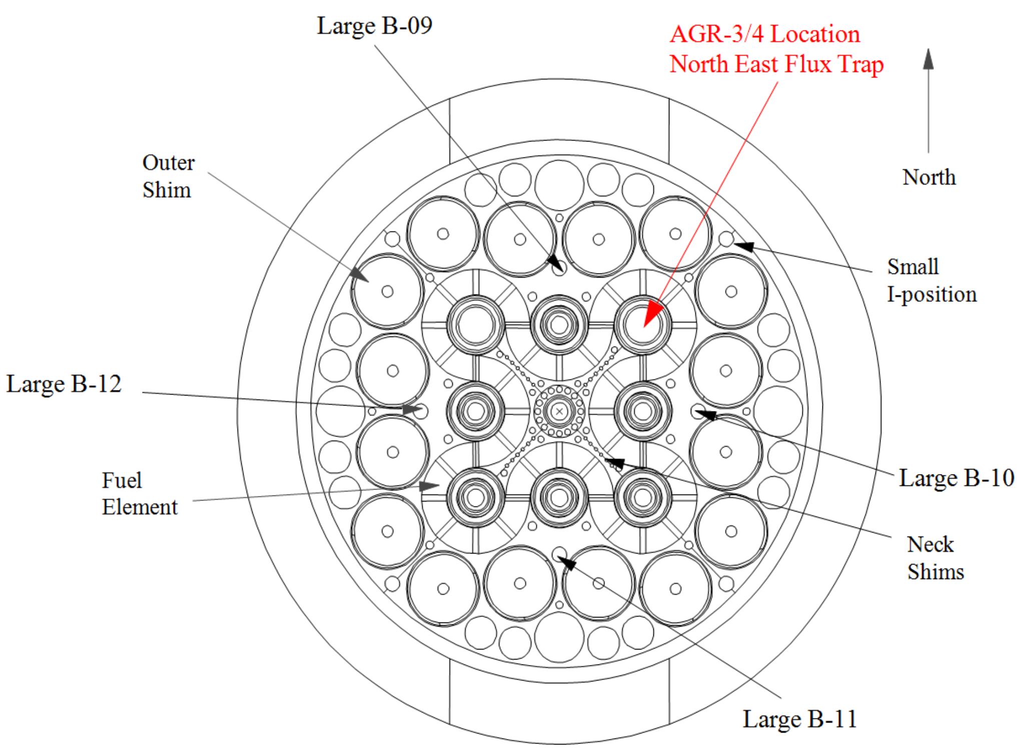

Figure 3. ATR core cross section displaying the NEFT position.

The AGR-3/4 test train was a multi-capsule, instrumented experiment that was designed for irradiation in the 133.4-mm diameter NEFT position of ATR. The best geometry for obtaining fission product transport data was determined to be a capsule that consists of a single stack of fuel compacts that contained a known fraction of DTF particles surrounded by three concentric annular rings of test material: (1) an annulus of fuel-compact matrix material; (2) an annulus of fuel-element graphite; and (3) an annulus of graphite operating at a lower temperature to act as a sink for fission products. This configuration best reduced axial thermal gradients and, hence, axial diffusion. The test reactor's axial flux distribution and space considerations within the test train imposed a practical limit of 12 independently controlled and monitored capsules per test train. An axial view of the test train is illustrated in Figure 4. Figure 5 illustrates the radial view of a capsule.

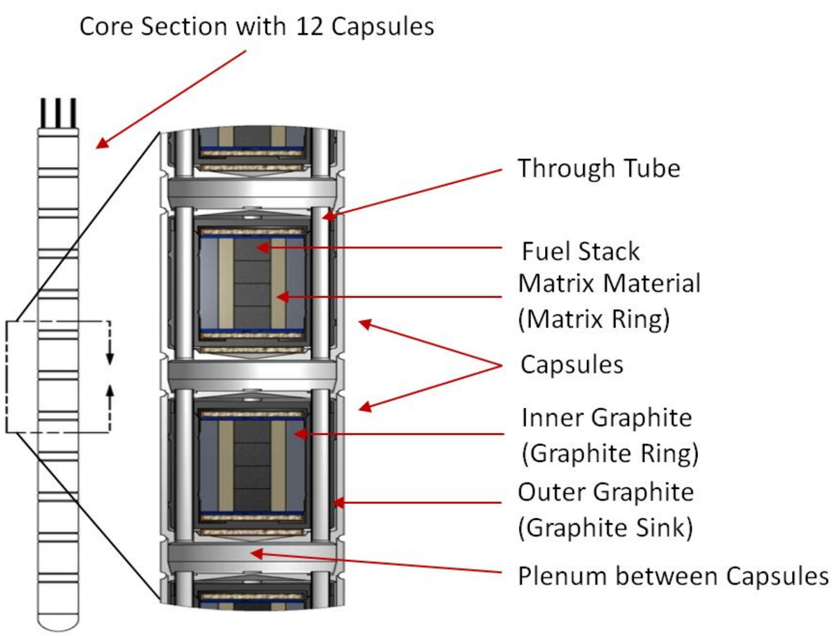

Figure 4. Axial schematic of the AGR-3/4 capsules.

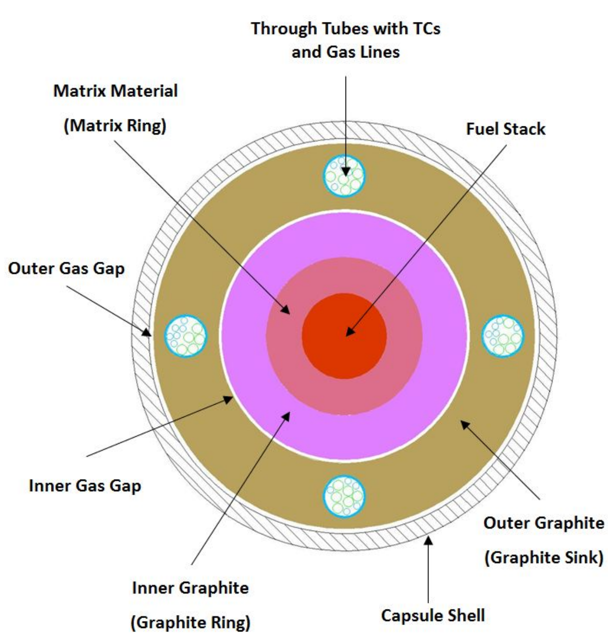

Figure 5. Radial schematic of the AGR-3/4 capsule.

2.3 AGR-3/4 Irradiation

AGR-3/4 was the third and fourth irradiation in the AGR program. Irradiation began in December 2011 and concluded in April 2014 in the B-12 position of the ATR for a total irradiation duration of 369.1 EFPD. Final burnup values on a per compact basis ranged from 4.85 to 15.27% FIMA, while fast fluence values ranged from 1.19 to 5.32 × 10^{25} n/m^2 (E_n > 0.18 MeV). TAVA fuel temperatures on a capsule basis at the end of irradiation ranged from 845°C in Capsule 12 to 1276°C in Capsule 7. The capsule-specific fluence, burnup, and TAVA temperatures used for this study is shown in Table 2 (Collin 2015).

Table 2. Capsule average thermal conditions and end-of-irradiation fluence and burnup.

Capsule	Average Fluence (× 10^{25} n/m^2) [E_n > 0.18 MeV]	Average Burnup (% FIMA)	TAVA (°C)
12	1.50	5.35	854
11	2.87	9.06	1226
10	3.94	11.81	1191
9	4.66	13.67	1008
8	5.08	14.52	1190
7	5.27	14.96	1345
6	5.31	15.24	1051
5	5.19	14.88	1015
4	4.85	14.21	1008
3	4.22	12.58	1177
2	3.21	10.07	1057
1	1.76	6.14	927

3. Bison MODELING

Using the data collected in the final as-run report (Collin 2015), Bison was used to model the AGR-3/4 experiment to determine the probability of fuel particle failure and the release fractions of the fission products silver (Ag), cesium (Cs), and strontium (Sr) to determine the source term for both the driver and DTF fuels. The analysis considered conventional fuel particle failure (i.e., typical pressure vessel failure) and multidimensional failure mechanisms (i.e., IPyC cracking and asphericity).

3.1 Boundary Conditions

Bison is designed to evaluate fuel performance based on user inputs for fast neutron fluence and burnup with a corresponding set of thermal conditions. The neutronics and thermal conditions for all the compacts used for comparison are based on results obtained from as-run neutronics calculations and as-run thermal analysis (Hawkes 2016; Sterbentz 2015).

Bison assumes all particles in a compact experience similar irradiation and thermal histories over the course of irradiation. Practically, Bison models one particle using the average burnup and fast neutron fluence and the volume-averaged temperature of the whole compact. In this scheme, Bison statistically treats a collection of particles within a range of geometrical dimensions and physical properties, but all the particles experience the same irradiation and thermal histories. For this analysis, capsule-specific fluence and burnup results from neutronics analyses performed previously and summarized in the AGR-3/4 final as-run report (Collin 2015) were used as inputs for the Bison analysis.

3.2 Input Parameters

Bison input parameters for modeling the AGR-3/4 experiment were taken from the AGR-3/4 Irradiation Test Final As-Run Report (Collin 2015). The fuel particle geometry and material properties are listed in Table 3 and Table 4, respectively. Three compacts were selected to analyze using Bison in this report. These compacts were selected based on the minimum TAVA temperature, peak TAVA temperature, and a compact that represents the average TAVA temperature experienced by all the compacts during irradiation. The irradiation conditions used in Bison for these compacts are summarized in Table 5. The as-run daily temperature profile is illustrated in Figure 6.

Table 3. Driver fuel particle geometry.

Attribute	Units	Mean Value	Standard Deviation
Kernel Diameter	µm	357.3	10.5
Buffer Thickness	µm	109.7	7.7
IPyC Thickness	µm	40.4	2.3
SiC Thickness	µm	33.5	1.1
OPyC Thickness	µm	41.3	2.1
Particle Sphericity	µm	1.056	--

Table 4. Driver fuel particle attributes.

Attribute	Units	Mean Value	Standard Deviation
Kernel Density	Mg/m^3	11.10	--
Buffer Density	Mg/m^3	1.10	--
IPyC Density	Mg/m^3	1.904	0.014
OPyC Density	Mg/m^3	1.901	0.012
IPyC BAF		1.027	0.002
OPyC BAF		1.021	0.002
PyC Poisson's Ratio in Creep		0.5	--
U-235 Enrichment	weight %	19.717	--
Oxygen-to-Uranium	atom ratio	1.430	--
Carbon-to-Uranium	atom ratio	0.361	--

Table 5. Irradiation conditions for selected compacts.

Capsule	Compact	Fluence ($\times 10^{25}$ n/m^2) [E_n > 0.18 MeV]	Burnup (% FIMA)	Time-Average Volume-Average Temperature (°C)	Notes
12	4	1.19	4.85	832	Minimum TAVA
7	3	5.27	15.00	1376	Peak TAVA
2	3	3.30	10.29	1081	Average TAVA

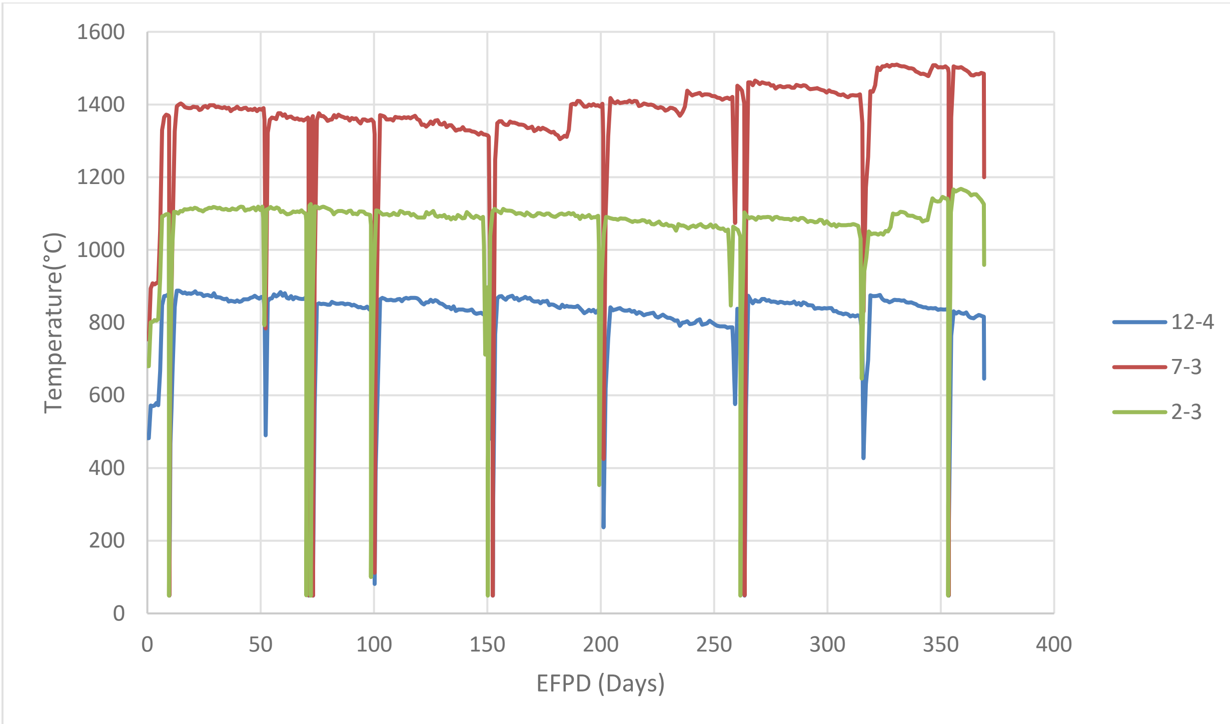

Figure 6. As-run temperature profile for selected compacts.

3.3 Multidimensional Stress

In addition to the one-dimensional (1D) behavior of a symmetrical spherical fuel particle, Bison considers multidimensional behavior, including cracking of the IPyC layer and aspherical geometry. Bison performs a two-dimensional (2D) simulation to obtain the effective mean strength and stress relationship of a particle with an IPyC crack or a faceted geometry based on the multidimensional stress distribution to make a statistical approximation of the stress levels in any particle (Jiang et al. 2021). These values are then used to modify the stress in the 1D solution to capture the multidimensional effects of IPyC cracking and asphericity.

3.4 Material Properties

Material properties used in Bison are similar to those discussed in great detail in the PARFUME Theory Manual and Model Basis Report (Miller 2018). Applications specific to Bison can be found in TRISO particle fuel performance and failure analysis with Bison (Jiang et al. 2021). The elastic moduli, swelling, thermal expansion, and thermal conductivity are treated as functions and the effective range for these properties extends to a fluence of 3.96×10^{25} n/m^2 (E_n >0.18 MeV) and between 600°C and 1300°C. However, an approximation was necessary to enable Bison modeling of some capsules in the AGR-3/4 test where the end-of-life fluence reaches as much as 5.31×10^{25} n/m^2. The approximation consists of treating the elastic moduli and swelling strain rates as constants in Bison beyond a fluence level of 3.96×10^{25} n/m^2 (E_n > 0.18 MeV).

The historical creep coefficient for the pyrocarbon layers (CEGA 1993) was found to be significantly lower than what has been used in other fuel performance models. It has also been found that previous fuel performance modeling has given favorable comparisons with results of the New Production - Modular High Temperature Gas Reactor experiments if the historical creep coefficient is approximately doubled (Miller et al. 2003). Therefore, the creep coefficient used in Bison in predictions for the AGR-3/4 test was set equal to twice the historical value.

3.5 Failure Analysis

A key metric of fuel performance is the extent of fuel particle failure during operation. The quality of the fuel can be characterized by how well the number of failures of the particles during reactor operation is minimized. Therefore, a performance model of the coating layers is needed to determine the failure probability of a population of fuel particles.

3.5.1 Failure Mechanisms

Three potential failure mechanisms are currently considered in Bison (Jiang et al. 2021). The first failure mechanism considered in Bison is a pressure vessel failure caused by buildup of gases (e.g., fission and CO). Initially, the SiC layer is in compression due to shrinkage of the pyrolytic carbon layers. As the irradiation progresses, the SiC compressive stress becomes relaxed due to the pyrolytic carbon creep and the accumulation of fission gas. If the buildup of fission gas is significant, all the layers are put in tension which can lead to a pressure vessel failure of the TRISO particle. In general, the CO production in a UCO fuel particle is not significant enough to cause a particle failure due to pressure (Ougouag, 2019) and was not considered in the Bison model.

The second failure mechanism currently considered in Bison is failure of the SiC layer caused by irradiation-induced shrinkage and the associated cracking of the IPyC layer. During irradiation, shrinkage of the initially intact IPyC layer induces a significant tensile stress in that layer. If the stress exceeds the tensile strength of the IPyC layer, then a radial crack develops in the IPyC. Because the shrinkage in the pyrocarbons dominates the particle behavior early during irradiation, large tensile stresses in the IPyC occur early. The presence of a crack in the IPyC layer creates a localized stress concentration in the SiC layer that could potentially lead to failure.

The third and final failure mechanism considered is pressure vessel failure that is impacted by particle asphericity. Aspherical particles have a flat facet created during fabrication but are otherwise spherical. During irradiation, the faceted portion of the particle acts as flat plate that restrains the internal gas pressure. If the pressure reaches a high enough value, a local region of tensile stress develops in the central portion of the plate that can contribute to particle failures. Unlike failures caused by cracking of the IPyC, which is governed by shrinkage of the pyrocarbons, failures caused by asphericity are dominated by the internal pressure. Therefore, while failures due to IPyC cracking are predicted to occur early during irradiation when shrinkage stresses are at their highest, failures due to asphericity are likely to occur later when the internal pressure is highest.

Other potential failure mechanisms (IPyC/SiC debonding, migration of the fuel kernel into the SiC layer, and chemical attack of the SiC layer by palladium) could be equally important and these are currently under development in Bison.

3.5.2 Weibull Statistical Distribution

Bison uses the Weibull statistical theory to determine whether the particle layers fail, using a mean strength for the IPyC layer and SiC layer based on a stress distribution corresponding to the failure mechanism under consideration. Bison compares the maximum calculated stress to a strength that is sampled from a Weibull distribution having mean strength and modulus. Weibull parameters that are used to evaluate failures of the SiC layer and cracking of the IPyC layer are discussed in the Combustion Engineering/General Atomics (CEGA) report (CEGA 1993).

4. RESULTS

Results from the AGR-3/4 test predictions were obtained using Bison and are based on the inputs and modeling parameters discussed previously. These results include fuel particle failure probability and fission product release fractions. The results of particle failure probability were obtained using the fast integration solver implemented in Bison. The fission product release calculations were run using the Monte Carlo scheme in Bison.

4.1 1D SiC Stress

The ability to produce accurate failure probability and fission product release predictions relies on the accuracy of the fuel performance tool on a simple 1D TRISO fuel particle. Bison results were compared to PARFUME to ensure both codes were producing similar results. The accumulation of internal particle pressure during irradiation can ultimately lead to a traditional pressure vessel failure of the particle if the stress in the SiC layer becomes greater than the mean strength of that layer. The Bison and PARFUME internal particle pressure for the three compacts are illustrated in Figure 7. In general, both codes were in good agreement. In addition, the amount of fission gas produced during irradiation is summarized in Figure 8. The two codes were in good agreement which is expected since they both use the same fission gas inventory correlation as a function of burnup. Since AGR-3/4 uses UCO fuel, it has previously been demonstrated that the buildup of CO is not sufficient for pressure vessel failure for this fuel form (Ougouag, 2019). Appendix A contains additional figures from the 1D Bison solution.

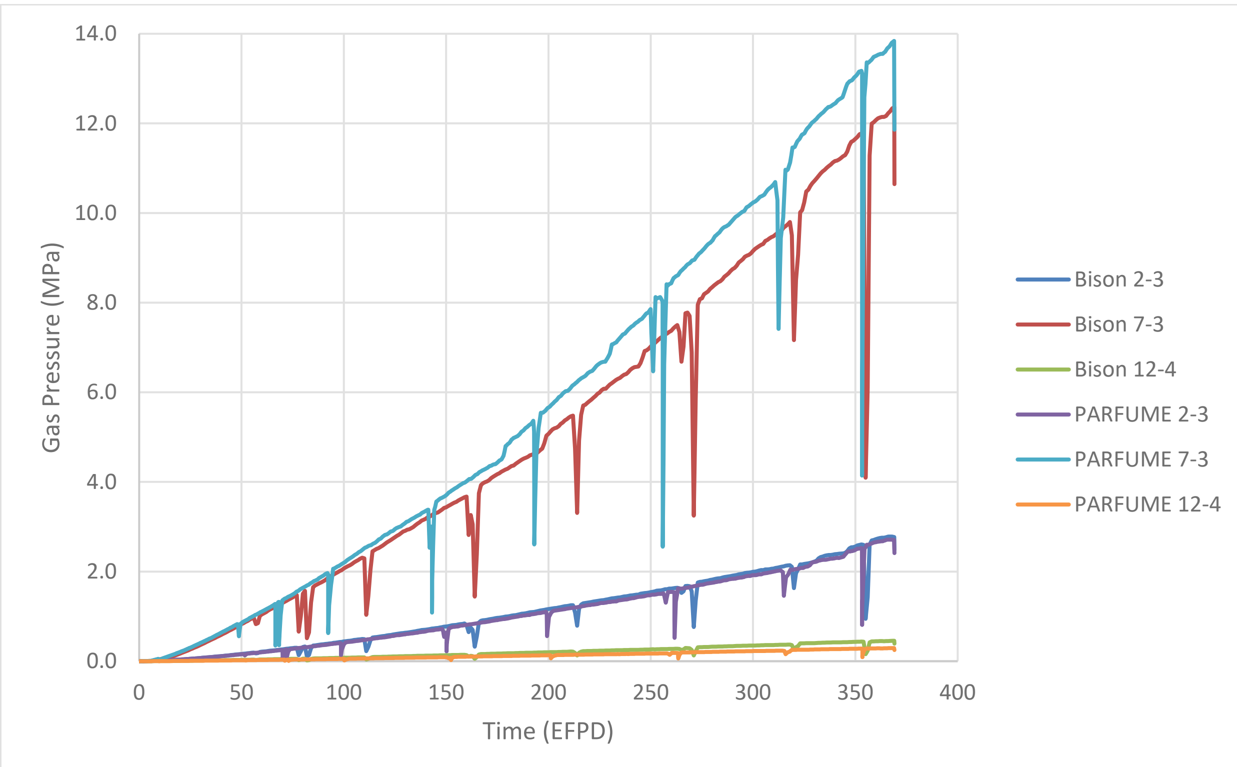

Figure 7. Internal gas pressure for selected AGR-3/4 compacts.

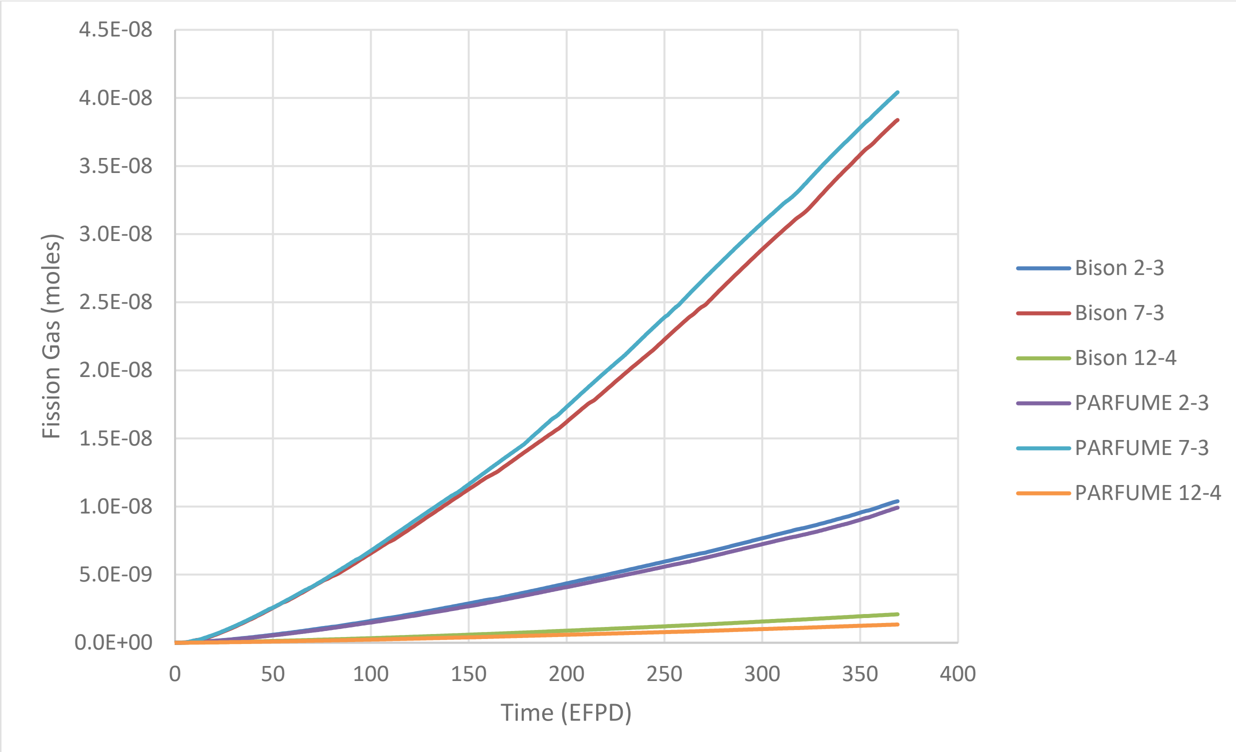

Figure 8. Fission gas produced for selected AGR-3/4 compacts.

The resulting 1D stress in the SiC layer for the two codes is illustrated in Figure 9. The SiC stress results experienced by a typical AGR-3/4 TRISO fuel particle throughout the duration of the irradiation were similarly predicted by both codes. The discrepancy between the two profiles in terms of where there are significant fluctuations in temperature are due to the larger time-steps in Bison. The Bison model uses time-steps in one day increments that are not discretized small enough to caption the power manipulations that occur mid time step. The stress profiles eventually converge at the end of irradiation and have no impact on the overall results, except for the timing of the potential fuel particle failures. The stress magnitude at these time/power fluctuations is also greater in Bison when compared to PARFUME. Future analyses will increase the number of time-steps in Bison to produce a more representative time/power evolution with smoother transitions between the discontinuities to eliminate the accentuated magnitude of the SiC stress profile.

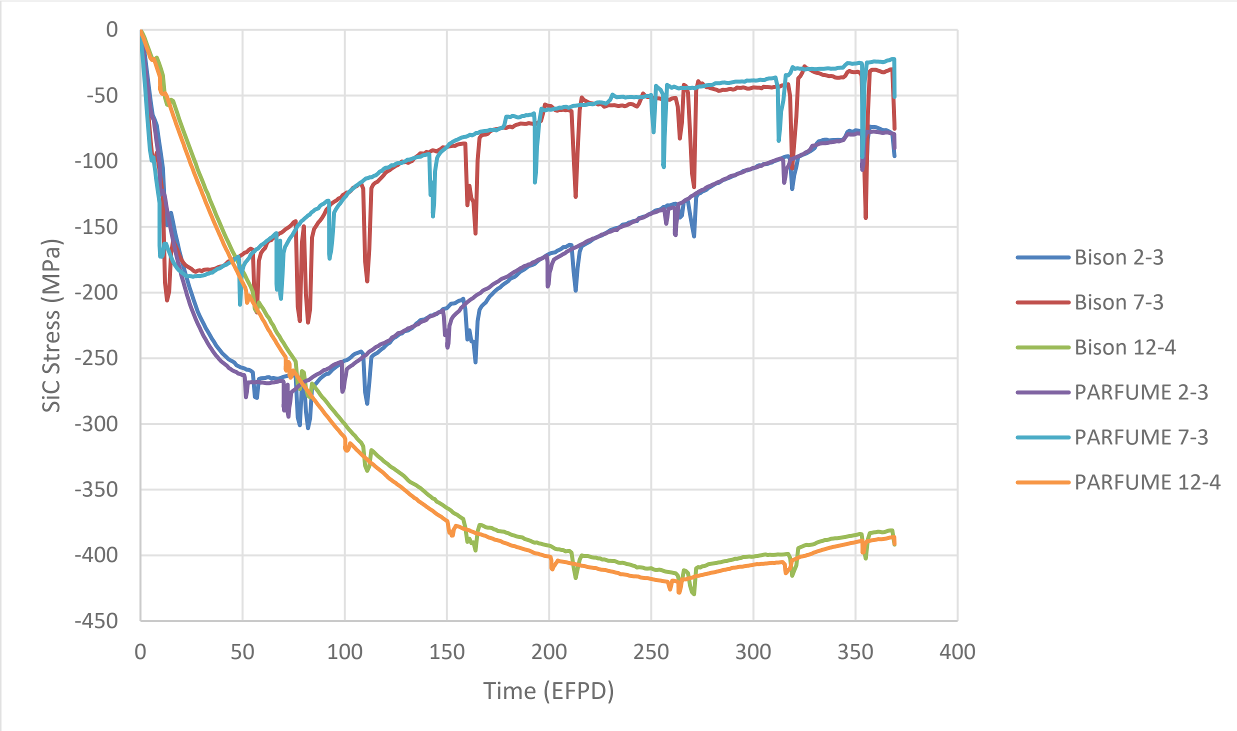

Figure 9. SiC layer stress for selected AGR-3/4 compacts.

4.2 Fuel Particle Failure Probability

It is assumed that a fuel particle has failed when the SiC layer has become compromised and cracked, which leads to its inability to retain fission products even if the OPyC layer may remain intact and able to retain fission gases. The primary mechanism leading to SiC cracking and subsequent fuel particle failure in the AGR-3/4 analyses is IPyC cracking. Complete results for the fuel particle failure probability analyses for the AGR-3/4 test using Bison are summarized with comparisons from PARFUME from a previous study (Skerjanc 2016) in Table 6. These results are illustrated in Figure 10.

Table 6. Fuel particle probability for Bison and PARFUME.

Compact	Fluence (10^{25} n/m^2)	Burnup (% FIMA)	TAVA (°C)	Probability of SiC Failure		
				PARFUME	Bison	Relative Difference
2-3	3.30	10.29	1081	1.56E-06	1.08E-02	6.91E+03
7-3	5.27	15.00	1376	3.55E-09	4.84E-03	1.36E+06
12-4	1.19	4.85	832	1.46E-04	3.90E-02	2.67E+02

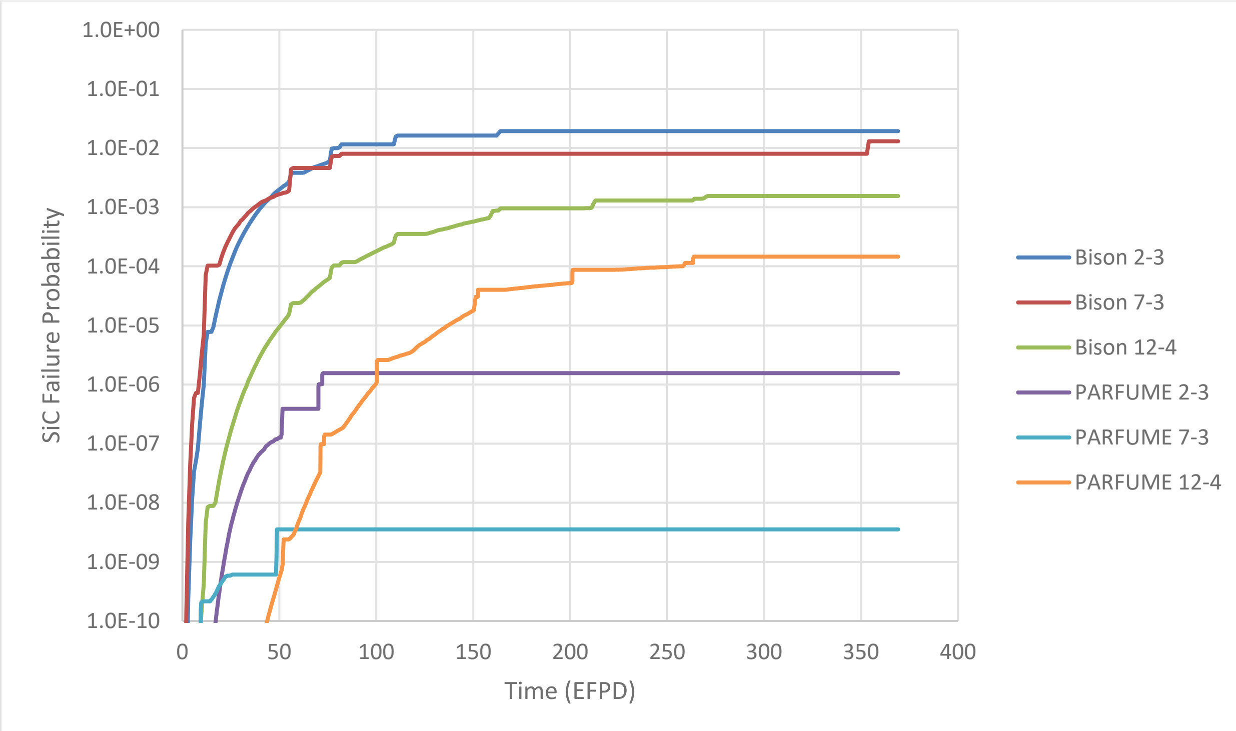

Figure 10. Fuel particle failure probability for selected AGR-3/4 compacts.

At first inspection, the Bison and PARFUME results are not in good agreement. This can be attributed to differences in the multidimensional strength and stress for a 2D solution of SiC failure associated with IPyC cracking. Bison uses the calculated strength and stress due to IPyC cracking at each time step, whereas PARFUME uses a generalized SiC strength and stress calculated by Abaqus using a TAVA temperature experienced throughout the irradiation. The SiC strength and stress associated with IPyC cracking used for both codes are summarized in Table 7. As Table 7 indicates, there is significant differences for the SiC strength and stress used by both codes.

Table 7. SiC strength and stress used for 2D solution for IPyC cracking.

Compact	Strength (MPa)		Stress (MPa)	
	Abaqus	Bison 2D	Abaqus	Bison 2D
2-3	1119	1447	194	751
7-3	1118	1383	134	654
12-4	1119	1455	268	941

When applying the Bison 2D calculated strength and stress in PARFUME, the results are in better agreement, as summarized in Table 8 and illustrated in Figure 11, but a significant discrepancy still exists.

Table 8. Failure probability using Bison 2D IPyC cracking strength and stress.

Compact	Fluence (10^{25} n/m^2)	Burnup (% FIMA)	TAVA (°C)	Probability of SiC Failure		
				PARFUME	Bison	Relative Difference
2-3	3.30	10.29	1081	1.10E-03	1.08E-02	8.80E+00
7-3	5.27	15.00	1376	1.35E-05	4.84E-03	3.59E+02
12-4	1.19	4.85	832	5.38E-02	3.90E-02	-2.76E-01

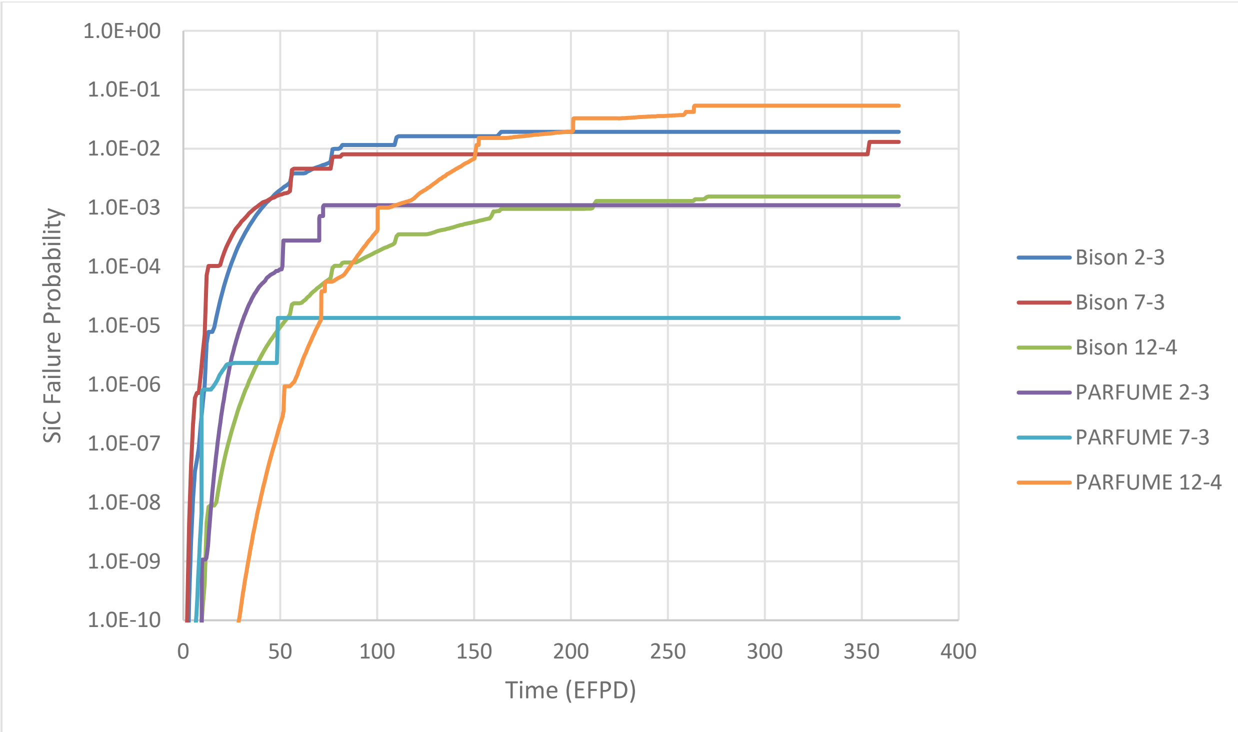

Figure 11. Fuel particle failure probability using Bison IPyC strength and stress.

Furthermore, when comparing the timing of the SiC failures in Bison versus the operation of the ATR during the irradiation, a significant increase in failure probability is observed during the power maneuvers. This is a result of the SiC stress being amplified during this time step, as illustrated in Figure 12 for compact 7-3. At approximately 80 EFPDs, the power maneuver results in a sudden increase of the SiC stress of ~125 MPa causing the SiC failure probability to suddenly increase. It is anticipated that a more continuous temperature/power evolution would result in Bison calculating a much lower failure probability. Using PARFUME and comparing the 2D Bison SiC stress before the power manipulation versus at the peak, (525 MPa versus 650 MPa), the failure probability decreases from 1.2×10^{-5} to 3.6×10^{-6}. An order of magnitude reduction in SiC failure probably is expected in Bison using a more continuous irradiation profile.

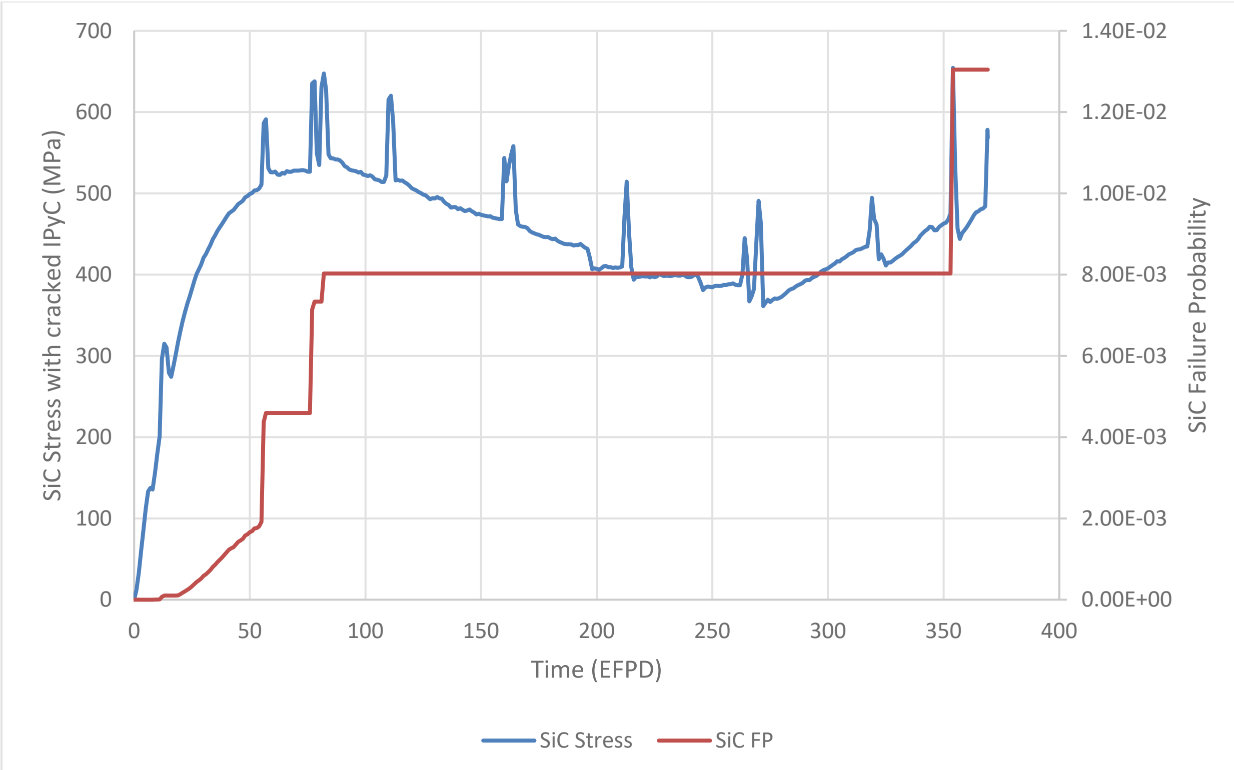

Figure 12. SiC stress and failure probability evolution for compact 7-3.

Finally, the historic pyrolytic creep data and subsequent correlations used in both Bison and PARFUME are based on temperatures above 600°C and may not be reliable during low power/temperature operation. During the AGR-5/6/7 irradiation experiment, zero fuel particle failures were detected while PARFUME predicted particle failures in the low-temperature compacts in Capsule 5 (Pham et al. 2021; Skerjanc 2021). As a result, an improved pyrolytic creep correlation for low temperatures is currently under investigation, and a more accurate model could decrease the predicted SiC failures for AGR-3/4. Currently for compacts 2-3, 7-3, and 12-4, Bison predicts 20, 9, and 73 driver fuel particle failures based on 1,872 fuel particles per compact. Based on actual performance during the AGR-3/4 irradiation, Bison greatly overpredicts the number of fuel particle failures. An updated pyrolytic creep model and eliminating the temperature/power discontinuities will reduce the number of predicted fuel particle failures by Bison during the AGR-3/4 irradiation test. The differences between Bison and the empirical data will be addressed in future analyses to improve the fidelity of the model.

4.3 Fission Product Release

4.3.1 Single Driver Fuel TRISO Particle

Bison was used to calculate the fission product release for silver (Ag), cesium (Cs), and strontium (Sr) for the three compacts using a single 1D TRISO driver fuel particle. A summary of the fission product release can be found in Table 9–Table 11 (for silver, cesium, and strontium, respectively), and the fission product release fraction for silver is illustrated in Figure 13.

Table 9. Ag release from a single TRISO driver fuel particle.

Compact	Released	Retained	Total	Release Fraction
2-3	5.98E-12	1.88E-10	1.94E-10	3.08E-02
7-3	2.99E-10	4.52E-11	3.44E-10	8.68E-01
12-4	4.80E-27	6.29E-11	6.29E-11	7.63E-17

Table 10. Cs release from a single TRISO driver fuel particle.

Compact	Released	Retained	Total	Release Fraction
2-3	1.44E-17	1.63E-08	1.63E-08	8.82E-10
7-3	1.34E-10	2.37E-08	2.38E-08	5.64E-03
12-4	2.72E-38	7.70E-09	7.70E-09	3.54E-30

Table 11. Sr release from a single TRISO driver fuel particle.

Compact	Released	Retained	Total	Release Fraction
2-3	1.11E-12	9.79E-09	9.79E-09	1.13E-04
7-3	1.76E-09	1.17E-08	1.35E-08	1.30E-01
12-4	-2.30E-29	5.12E-09	5.13E-09	0.00E+00

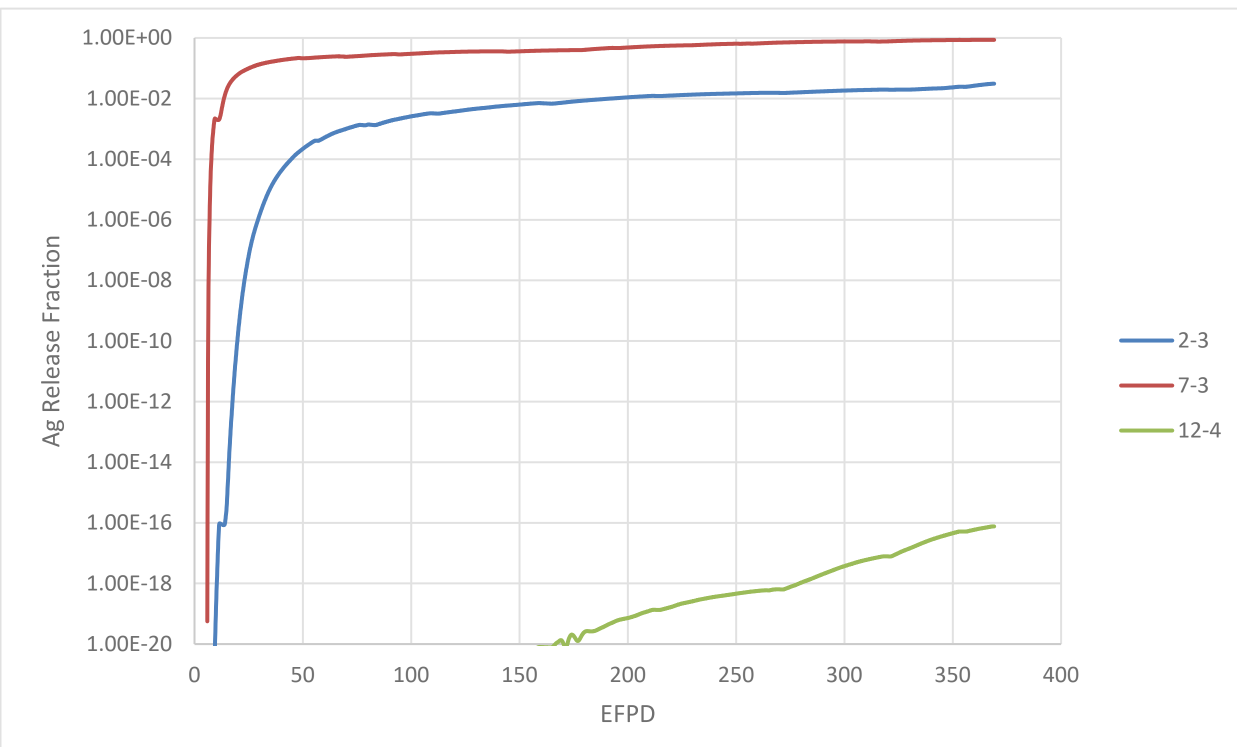

Figure 13. Ag release fraction from a single TRISO driver fuel particle.

4.3.2 Compact Fission Product Release

Each AGR-3/4 compact contained driver fuel particles and 20 DTF particles placed along its axial centerline. The fuel compacts are surrounded by three concentric annular rings of test material consisting of fuel-compact matrix material and fuel-element graphite. Figure 14 shows a Bison 2D axisymmetric model, with the 20 DTF particles placed in the center line and 1793 randomly distributed driver particles hosted in the fuel compact. The four regions of the Bison model are fuel compact, matrix, graphite, and the sink. They are separated blocks without sharing nodes between their interfaces. Their height is 12.5 mm and wall thicknesses are 6.15 mm, 6.05 mm, 6.3 mm, and 13.14 mm, respectively. The physical properties of the TRISO fuel particle including kernels and coating layers are randomly generated from a Monte Carlo simulation. At every time step, the fission product and heat released from each particle is transferred to the compact as a point source. Those point sources are used in the compact model to drive the fission product and thermal diffusion. In this 2D axisymmetric model, the point sources are treated as circular sources.

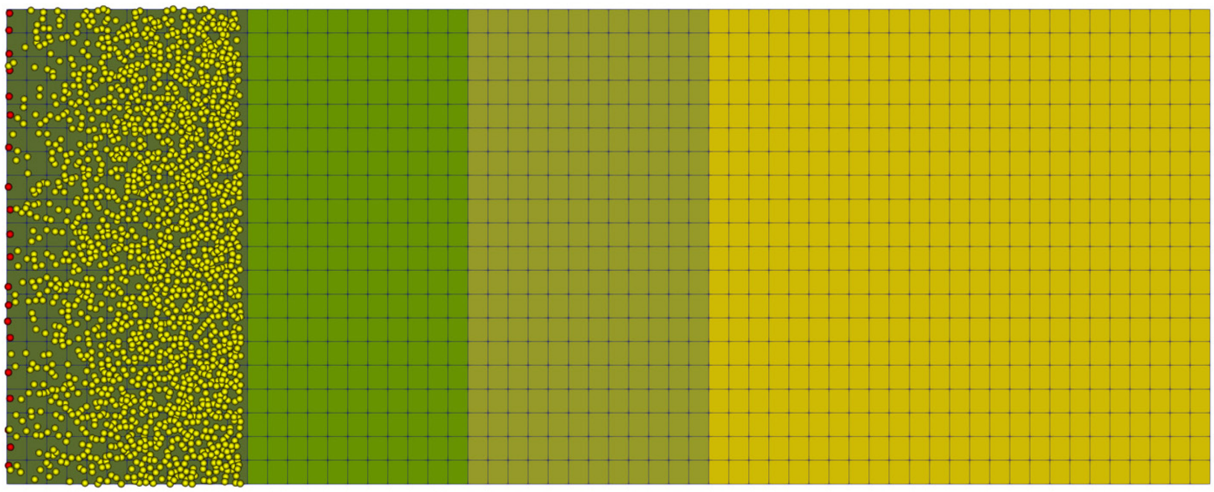

Figure 14. Bison 2D axisymmetric model of fission product transport. The four regions of the Bison model are fuel compact, matrix, graphite, and sink. 20 DTF particles are placed in the center line and 1793 driver fuel particles are randomly generated from Monte Carlo simulation in the compact region.

The cesium and thermal diffusion in compact 12-4 were simulated. The Arrhenius diffusion coefficients of cesium are listed in Table 12. The fuel compact temperature in compact 12-4 is controlled at 900 °C. The inner and outer temperature boundary conditions are set for each block using the values listed in Table 13. The temperature profile solved by Bison at 100 days is shown in Figure 15. In addition to the discontinuities in temperature, the presence of gaps also results in discontinuities of fission product concentration. The interfacial conditions of fission product diffusion are derived in (INL 2015) based on the sorption isotherm theory. In this work, the fission product concentrations are enforced to be continuous cross block gaps using a penalty method. The discontinuous interfacial conditions will be implemented in the future.

Table 12. Arrhenius diffusion coefficients of Cesium.

Material	D_0 [m^2/s]	Q[J/mol]
Matrix	3.60×10^{-4}	189000
Graphite	1.70×10^{-6}	149000

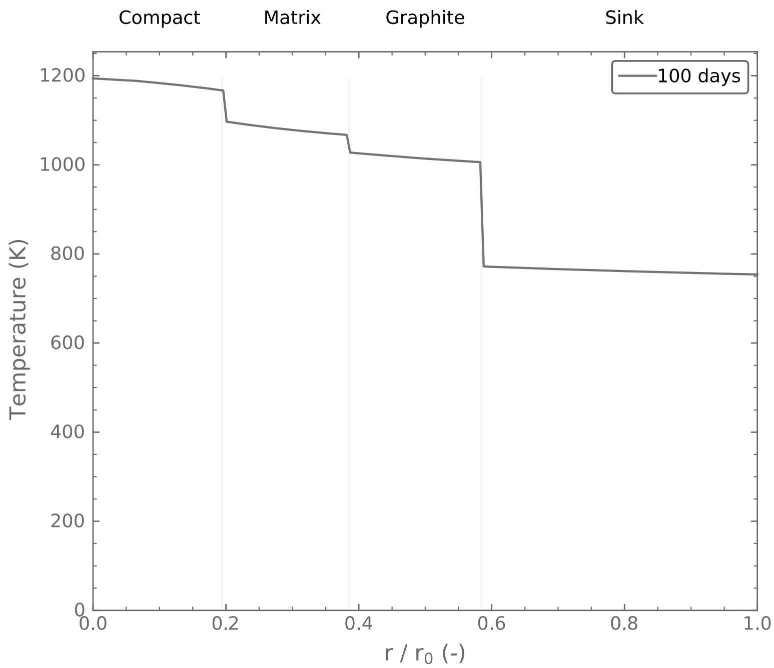

Figure 15. Temperature profile at 100 days.

Table 13. Temperature boundary conditions.

Compact	Matrix		Graphite		Sink	
Outer Temp	Inner Temp	Outer Temp	Inner Temp	Outer Temp	Inner Temp	Outer Temp
893 °C	824 °C	794 °C	755 °C	733 °C	499 °C	481 °C

The cesium concentration at 100, 200 and 300 days of the simulation is shown in Figure 16. The 2D contour shows that the primary source of cesium comes from the DTF particles by setting the diffusivities to a large value. The failure probability of the driver fuel is not coupled with the fission product diffusion model but will be considered in the future. Most of the cesium is retained in the compact because of its relatively low diffusion coefficients. Since the graphite has even a lower diffusion coefficient, there is almost no transport through the graphite and the sink.

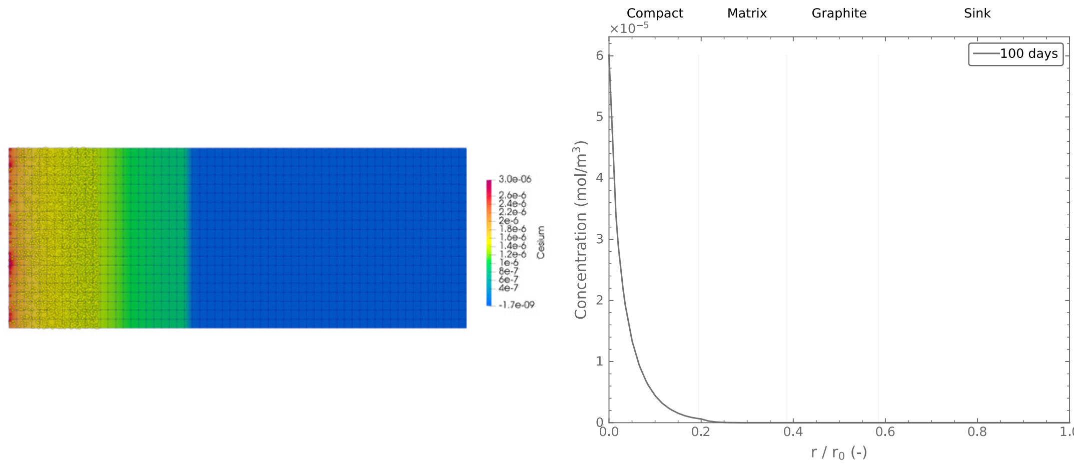

(a) 100 days

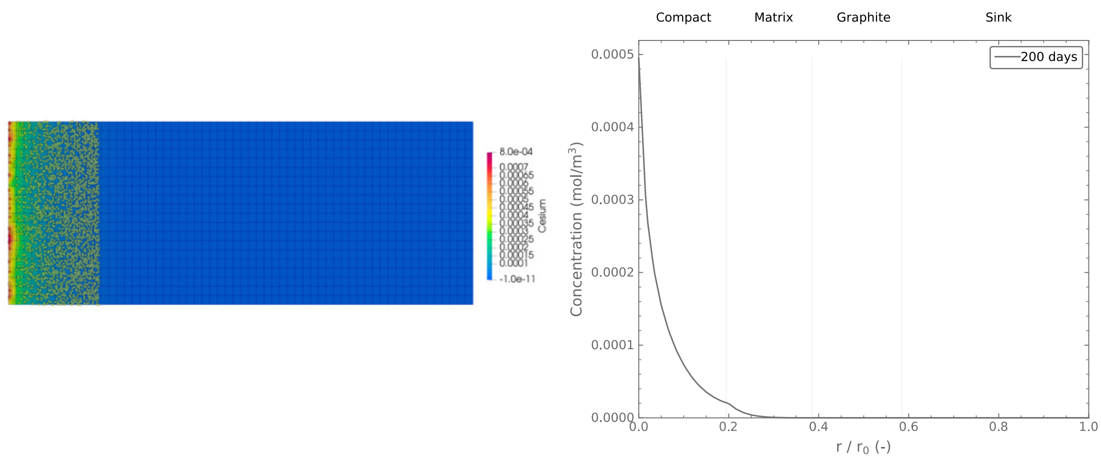

(b) 200 days

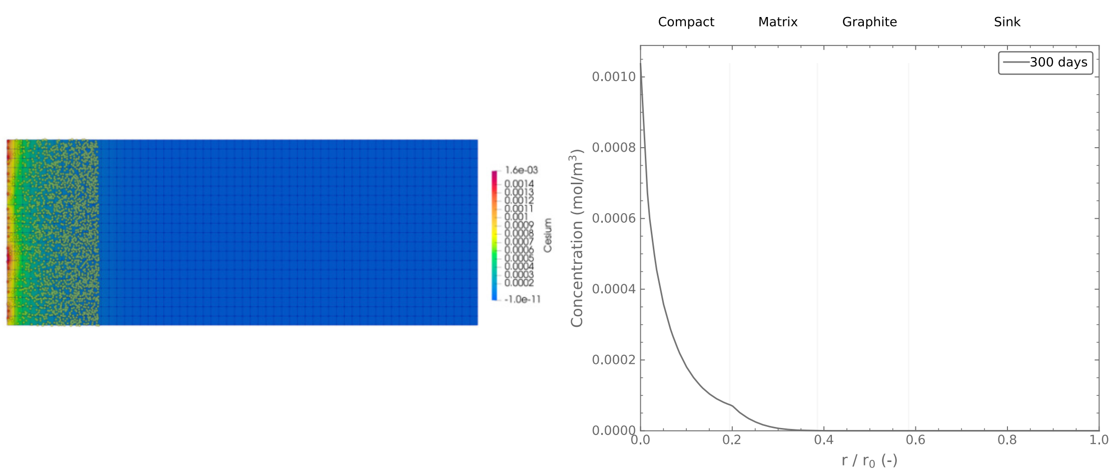

(c) 300 days

Figure 16. Cesium profile at (a) 100 days; (b) 200 days; (c) 300 days.

5. CONCLUSION

Fuel particle failure analysis was completed using Bison to analyze the failure probability of driver fuel particles in selected compacts during the AGR-3/4 irradiation test. Using as-run neutronic physics and thermal hydraulic data, the fuel particle failure probability, fission product release from the driver fuel and DTF particles have been analyzed for the selected compacts. The following summarizes the results derived from this work.

Although the 1D simulations of an AGR-3/4 driver fuel particle performance were in good agreement between Bison and PARFUME, significant discrepancies existed between the two codes when considering the 2D effects of a cracked IPyC layer on the localized stress in the SiC layer. This can be attributed to the different multidimension stress and strength inputs used between the two codes. When applying the Bison 2D strength and stress values in PARFUME, the codes were in much better agreement. Furthermore, the high calculated SiC failure probability by Bison can be attributed to two factors:

1) The temperature/power evolution of the ATR during the irradiation test results in a discontinuous temperature/power profile from the large operational changes during shutdowns. Temperatures can go from 1050° to 50°C in a matter of a couple of EFPDs causing unrealistically large 2D SiC stress levels in the layer due to IPyC cracking. In addition, some of the models used in Bison are not valid below 600°C resulting in unrealistic failure probabilities. Removing the discontinuity during the power evolutions in the temperature/power profile will result in lower SiC failure fractions and more accurately model the fuel performance in future analyses.
2) Historic data for creep in pyrolytic carbon and the resulting correlations used in Bison at lower temperatures is suspect and results in higher than expected SiC layer failures. This issue has been demonstrated during the AGR-5/6/7 irradiation test and subsequent fuel particle failure probabilities calculated by PARFUME.

These two factors will be addressed prior to performing the AGR-3/4 as-run calculations by Bison for each compact and subsequent use in comparison to the PIE data. Additionally, fission product concentrations are continuous across block gaps using a penalty method. The discontinuous interfacial conditions will be implemented in the future to model the fission product diffusion more accurately to the graphite sink.

6. REFERENCES

Barnes, C. M., 2006a, "AGR-1 Fuel Product Specification and Characterization Guidance," EDF-4380, Rev. 8, Idaho National Laboratory.

Barnes, C. M., 2006b, "AGR-3 & 4 Fuel Product Specification," EDF-6638, Rev. 1, Idaho National Laboratory.

BWXT, 2006, "Industrial Fuel Fabrication and Development Lot G73V-20-69303," Data Certification Package, BWX Technologies.

CEGA Corporation, 1993, "NP-MHTGR Material Models of Pyrocarbon and Pyrolytic Silicon Carbide," CEGA-002820, Rev.1, CEGA Corporation.

Collin, B. P., 2015, "AGR-3/4 Irradiation Test Final As-Run Report," INL/EXT-15-35550, Rev. 1, Idaho National Laboratory.

Demkowicz, P. A., 2021, "Technical Program Plan for INL Advanced Reactor Technologies Advanced Gas Reactor Fuel Development and Qualification Program," PLN-3636, Rev. 10, Idaho National Laboratory.

Hales, J. D., "Bison TRISO Modeling Advancements and Validation to AGR-1 Data," INL/EXT-20-59368, Rev. 0, Idaho National Laboratory, September 2020.

Hawkes, G. L., 2016, "AGR-3/4 Daily As-Run Thermal Analyses," ECAR-2807, Rev. 1, Idaho National Laboratory.

Hunn, J. D., 2007, "Data Compilation for AGR-3/4 Driver Fuel Coated Particle Composite LEU03-09T," ORNL/TM-2007/019, Oak Ridge National Laboratory.

Hunn, J. D., 2011, "Data Compilation for AGR-3/4 Designed-To-Fail (DTF) Fuel Particle Batch LEU03-07DTF," ORNL/TM-2011/109, Oak Ridge National Laboratory.

INL, 2015, "AGR-3/4 Irradiation Experiment Test Plan", INL/MIS-11-22351.

Jiang, W., J. D. Hales, B. W. Spencer, B. P. Collin, A. E. Slaughter, S. R. Novascone, A. Toptan, K. A. Gamble, R. Gardner, 2021, "TRISO particle fuel performance and failure analysis with Bison," Journal of Nuclear Materials 548: 152795. https://doi.org/10.1016/j.jnucmat.2021.152795.

Maki, J. T., 2011, "AGR-3/4 Irradiation Test Specification," SPC-1345, Idaho National Laboratory.

Marshall, D. W., 2011, "AGR-3/4 DTF Fuel and Capsule Component Material Specifications," SPC-1214, Rev. 1, Idaho National Laboratory.

Miller, G. K., D. A. Petti, D. J. Varacalle Jr., and J. T. Maki, 2003, "Statistical approach and benchmarking for modeling of multi-dimensional behavior in TRISO-coated fuel particles," Journal of Nuclear Materials 317: 69–82.

Miller, G. K., D. A. Petti, J. T. Maki, D. L. Knudson, W. F. Skerjanc, 2018, "PARFUME Theory and Model Basis Report," INL/EXT-08-14497, Rev. 1, Idaho National Laboratory.

Ougouag, A., C. Jiang, 2019, "CO Production Model Analysis for Correlations into PARFUME," ECAR-4734, Rev. 0, Idaho National Laboratory.

Permann, C. J., D. R. Gaston, D. Andrš, R. W. Carlsen, F. Kong, A. D. Lindsay, J. M. Miller, J. W. Peterson, A. E. Slaughter, R. H. Stogner, and R. C. Martineau, 2020, "MOOSE: Enabling massively parallel multiphysics simulation," SoftwareX 11: 100430. https://doi.org/10.1016/j.softx.2020.100430.

Pham, B. T., J. Palmer, D. W. Marshall, G. L. Hawkes, D. M. Scates, and P. A. Demkowicz, 2021, "AGR-5/6/7 Irradiation Test Final As-Run Report," INL/EXT-21-64221, Rev. 0, Idaho National Laboratory.

Skerjanc, W. F., 2016, "AGR-3/4 Irradiation Test Predictions Using PARFUME," INL/EXT-16-38280, Rev. 0, Idaho National Laboratory.

Skerjanc, W. F., 2021, "AGR-5/6/7 Irradiation As-Run Predictions Using PARFUME," INL/EXT-21-64567, Rev. 0, Idaho National Laboratory.

Sterbentz, J. W., 2015, "JMOCUP As-Run Daily Physics Depletion Calculation for the AGR-3/4 TRISO Particle Experiment in ATR Northeast Flux Trap, ECAR-2753, Rev. 1, Idaho National Laboratory.

Williamson, R. L, J. D. Hales, S. R. Novascone, G. Pastore, K. A. Gamble, B. W. Spencer, W. Jiang, S. A. Pitts, A. Casagranda, D. Schwen, A. X. Zabriskie, A. Toptan, R. Gardner, C. Matthews, W. Liu, and H. Chen , "BISON: A Flexible Code for Advanced Simulation of the Performance of Multiple Nuclear Fuel Forms", Nuclear Technology, 2021, 207:7, 954 - 980, DOI: 10.1080/00295450.2020.1836940

Page intentionally left blank

Appendix A
1D Bison Modeling Data

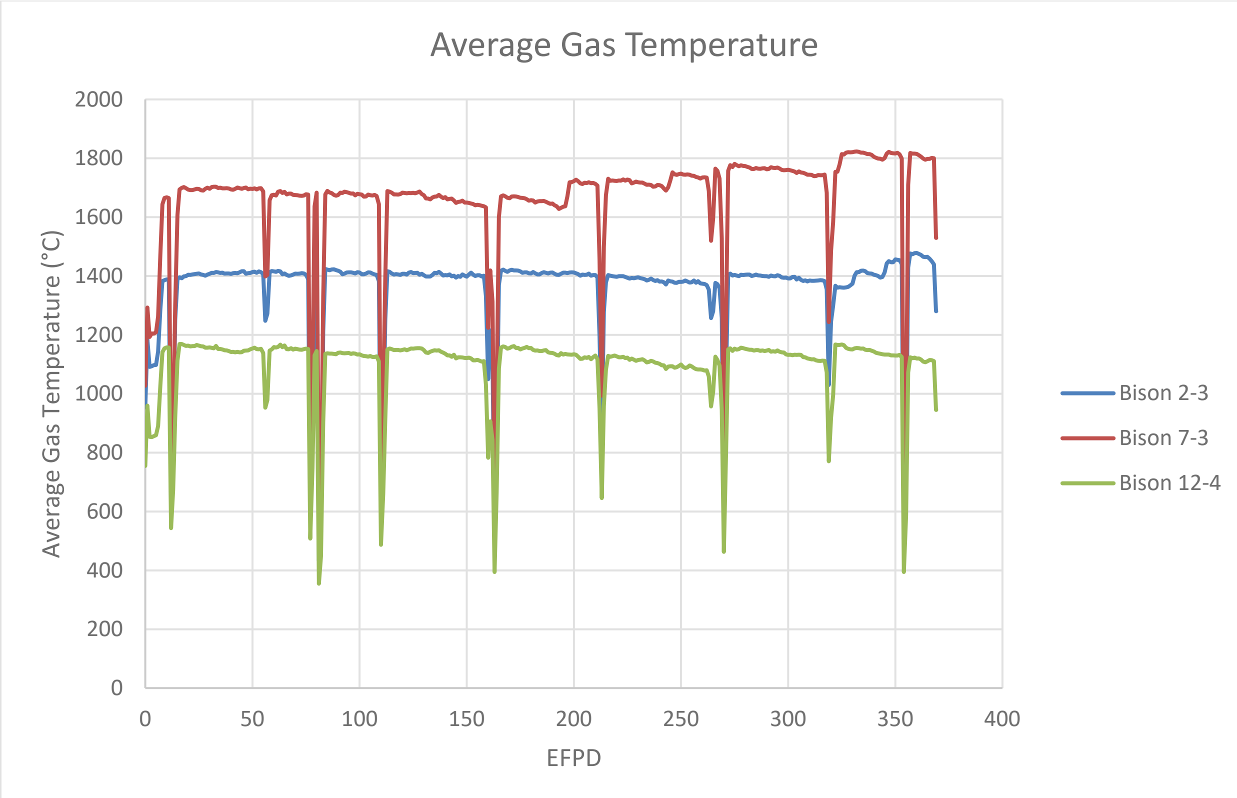

Figure A1. Average compact gas temperature.

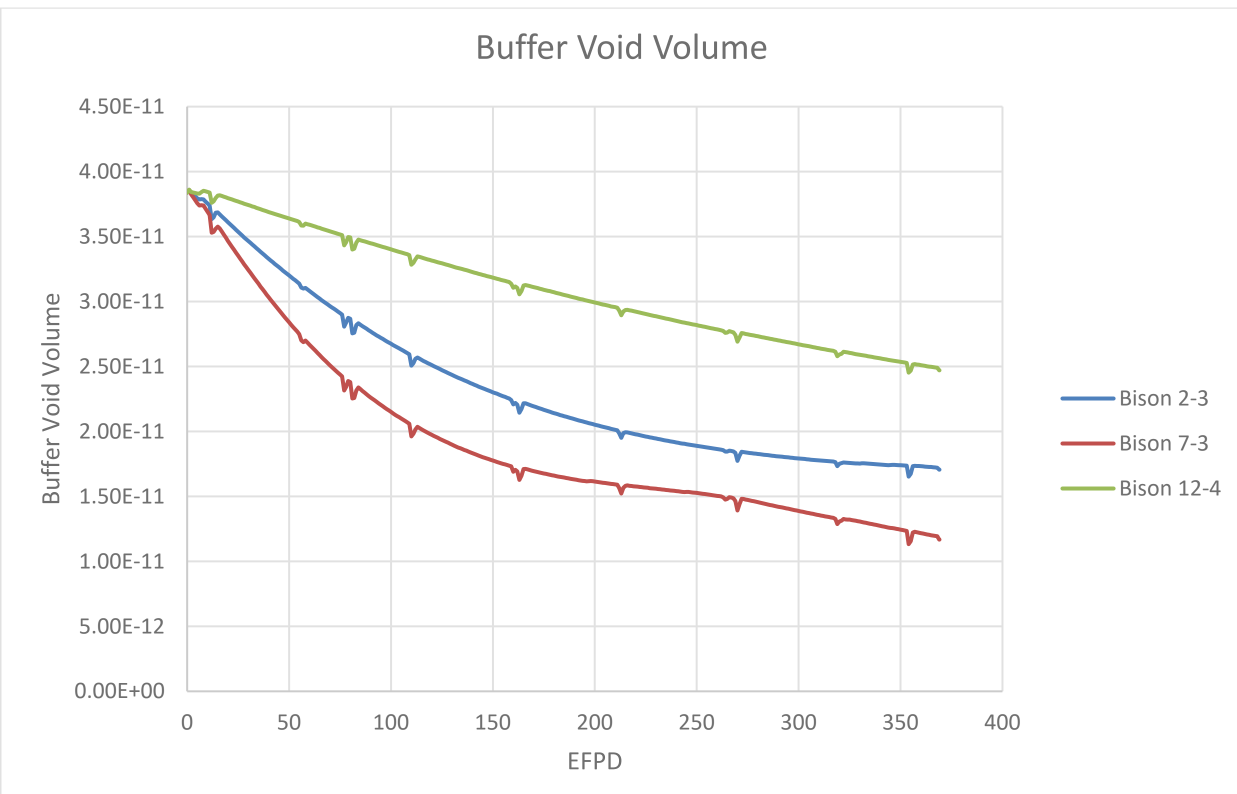

Figure A2. Buffer void volume.

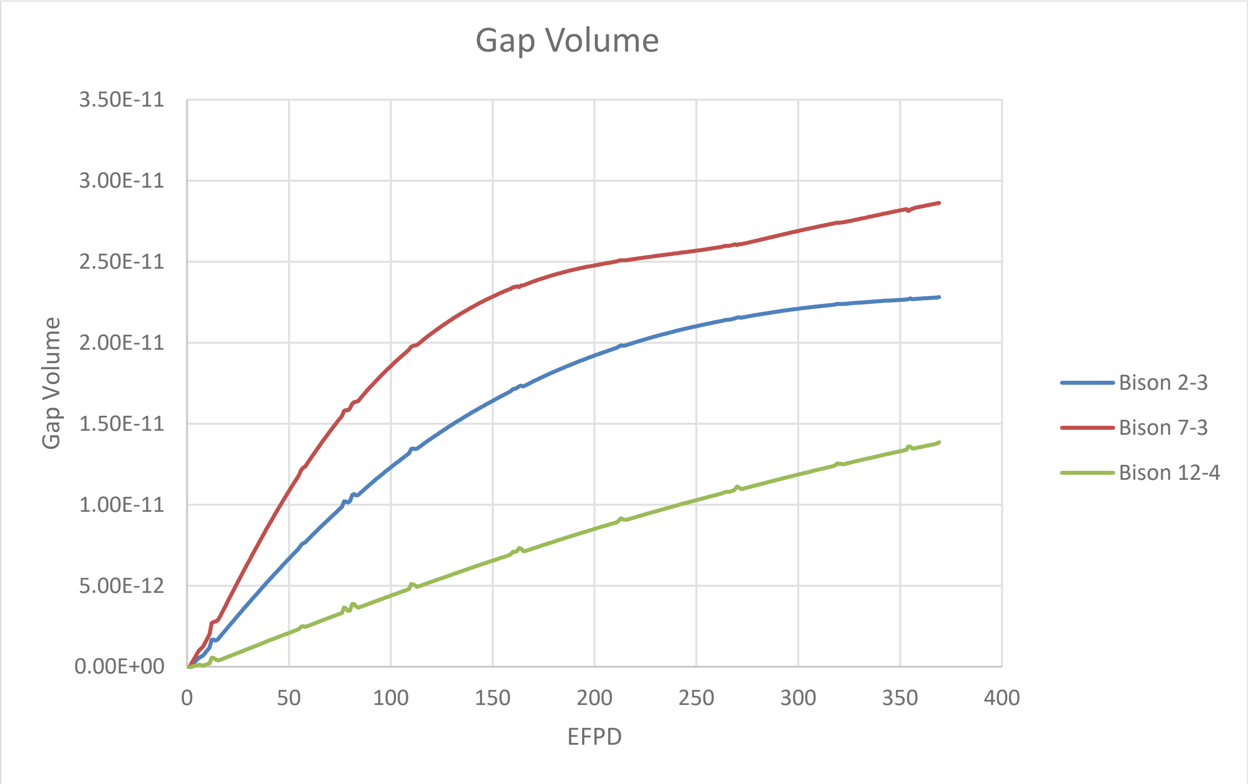

Figure A3. Gap volume.

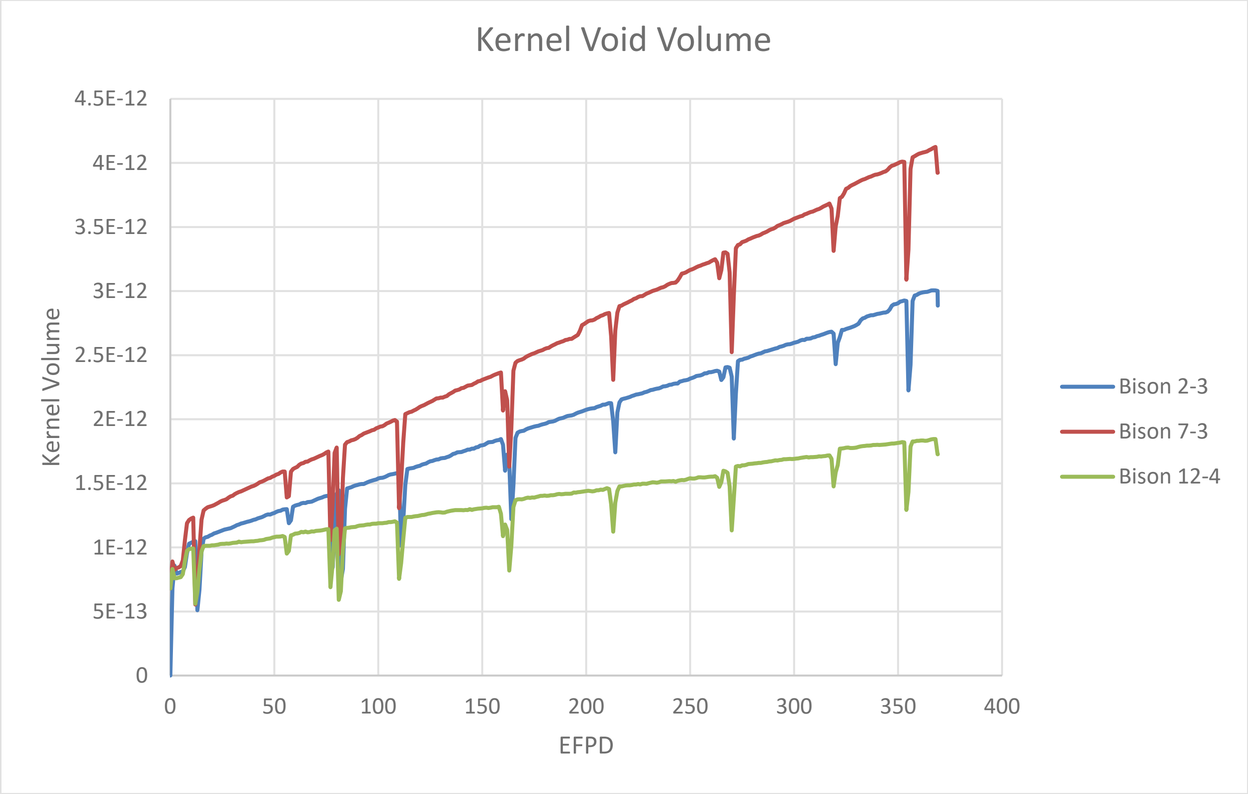

Figure A4. Kernel void volume.